Diffusion-controlled cluster formation in 2–6-dimensional space

Paul Meakin
Experimental Station, Central Research and Development Department, E. I. du Pont de Nemours and Company, Inc., Wilmington, Delaware 19898
(Received 16 November 1982)

Diffusion-controlled cluster formation has been simulated on lattices of dimensionality 2–6. For the case of a sticking probability of 1.0 at nearest-neighbor sites, we find that the radius of gyration (R_g) of the cluster is related to the number of particles (N) by $R_g \sim N^{\beta}$ (for large N). The exponent β is given by $\beta \sim 6/5d$, where d is the classical (Euclidean) dimensionality of the lattice. These results indicate that the Hausdorff (fractal) dimensionality (D) is related to the Euclidean dimensionality (d) by $D \approx 5d/6$ ($d = 2$–6). Similar results can be obtained from the density-density correlation function in two-dimensional simulations. Nonlattice simulations have also been carried out in two- and three-dimensional space. The radius-of-gyration exponents (β) obtained from these simulations are essentially equal to those obtained in the lattice model simulations. We have also investigated the effects of sticking probabilities (S) less than 1.0 on diffusion-limited cluster formation on two- and three-dimensional lattices. While smaller sticking probabilities do lead to the formation of denser clusters, the radius-of-gyration exponents are insensitive to sticking coefficients over the range $0.1 \leq S \leq 1.0$.

INTRODUCTION

The aggregation of particles to form flocs or clusters has, for a long time, been one of the central phenomena in colloid science with important implications for problems such as the control of water and air pollution,[1] as well as for a very wide variety of natural and commercial processes. The importance of this problem has stimulated a large amount of research including computer simulations of floc formation by Vold[2] and Sutherland *et al.*[3] While this early work did include some of the effects of Brownian motion by allowing single particles or clusters of particles to approach each other from random directions and with random orientations, the most important effects of Brownian motion on cluster formation have only recently been revealed by the work of Witten and Sander.[4] By means of Monte Carlo simulations, Witten and Sander have demonstrated that diffusion-controlled growth on a "seed" particle in two-dimensional space results in a cluster which has an associated fractal[5] (Hausdorff[6]-Besicovitch) dimensionality of about $\frac{5}{3}$ in the limit of large cluster size. We have recently confirmed the results of Witten and Sander and obtained similar results for diffusion-controlled cluster formation in three- and four-dimensional space.[7]

Besides its importance in understanding aggregation phenomena in colloidal systems and other dispersions, diffusion-controlled cluster formation provides a relatively simple limiting case model for other important phenomena such as dendritic growth and polymerization processes.

In the present paper we present additional information concerning the nature of clusters formed by

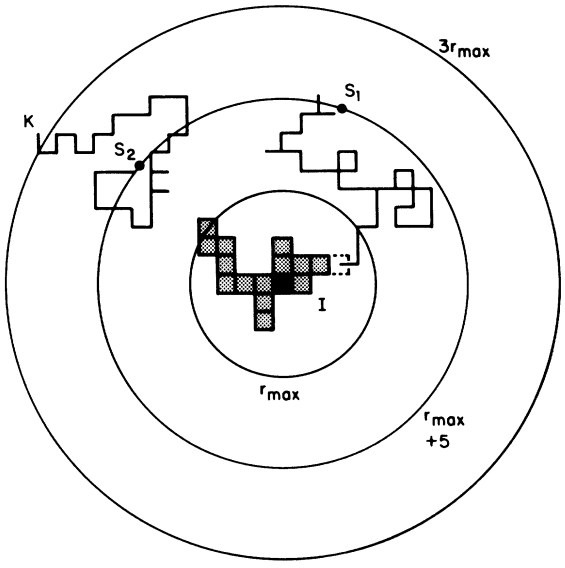

FIG. 1. Monte Carlo simulation of diffusion-controlled cluster formation using a two-dimensional lattice model.

diffusion-controlled processes in two-, three-, and four-dimensional space together with results obtained from Monte Carlo simulations in five- and six-dimensional space. Because cluster formation in three-dimensional space is the most important from a practical point of view, this is one of the major focuses for the present paper. However, cluster formation in two-dimensional systems (surfaces) is also of importance and is discussed in detail. Cluster formation in four-dimensional space and spaces of higher dimensionality has less physical significance. However, results obtained from simulations in higher dimensionalities should lead to a better overall understanding of diffusion-controlled cluster formation and its relationship to phenomena such as polymer gelation,[8,9] percolation,[10] and other critical phenomena.[11]

Results obtained for similar simulations of diffusion-controlled deposition on surfaces and linear nucleation sites (fibers) will be presented in a separate paper.

FIG. 2. Two-dimensional cluster of 11 260 particles obtained using the procedure illustrated in Fig. 1 and described in more detail in the text. Sticking coefficient is 1.0 at nearest-neighbor positions.

TWO-DIMENSIONAL CLUSTERS

The simulation of diffusion-controlled cluster formation in two-dimensional space has been described by Witten and Sander.[4] Witten and Sander start with a single seed particle at the origin of a lattice. A second particle is added a long distance from the origin and undergoes a random walk on the lattice until it reaches a site adjacent to the seed and becomes part of the growing cluster. If the particle reaches a position which is very far from the seed particle, it is "killed" and started off again at a randomly chosen position closer to the seed and the random walk is continued. Eventually, the particle reaches a position adjacent to the seed and becomes part of the cluster. A third particle is then introduced at a random distant point and undergoes a random walk until it also becomes incorporated into

TABLE I. Results obtained from simulations of diffusion-controlled cluster formation on two-dimensional square lattices with a sticking probability of 1.0 at nearest-neighbor sites.

Number of particles for cluster	Radius-of-gyration exponent (β) 50%[a]	75%[b]	90%[c]	95%[d]	Density-density correlation function exponent (α)	Average coordination number
11 062	0.577	0.576	0.587	0.587	0.273	2.193
11 806	0.582	0.583	0.570	0.569	0.294	2.185
10 240	0.590	0.610	0.604	0.605		2.183
7 740	0.552	0.568	0.588	0.595		
7 731	0.599	0.602	0.607	0.608	0.367	2.198
9 658	0.599	0.615	0.611	0.612	0.348	2.197
8 827	0.545	0.561	0.568	0.566	0.329	2.188
Avg. 8 585	0.578±0.020	0.588±0.020	0.591±0.016	0.592±0.017	0.322±0.047	2.191±0.007

[a]Last 50% of clusters formed.
[b]Last 75% of clusters formed.
[c]Last 90% of clusters formed.
[d]Last 95% of clusters formed.

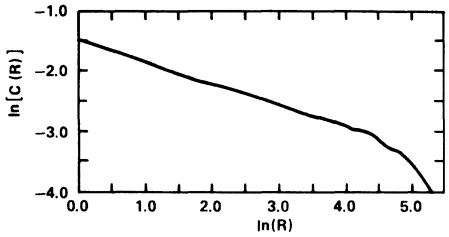

FIG. 3. Density-density correlation function calculated for the cluster shown in Fig. 2.

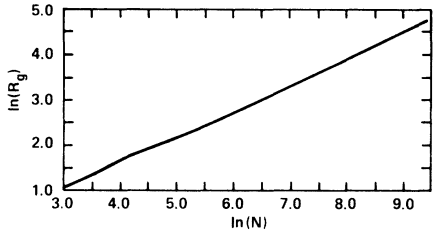

FIG. 4. Dependence of radius of gyration on cluster size during the growth of a cluster of 12 723 particles under the conditions used to obtain Figs. 2 and 3.

the growing cluster. The procedure is repeated until a cluster of sufficiently large size is formed.

Some additional details of our simulation procedure, including methods used to reduce computer time requirements, are described in this section. Since a particle undergoing a random walk starting from a point a large distance from the cluster will intersect a circle enclosing the cluster, for the first time, at a point at random on the circle we start the particle out at a random point on a circle centered on the seed particle with a radius slightly (about 5 lattice spacings) larger than the distance from the seed to the most distant particle in the cluster (the maximum radius of the cluster, r_{max}; see Fig. 1). The particle is then moved to the nearest lattice site. If the particle reaches a point more than three times the maximum radius of the cluster from the origin, it is killed and a new particle is started. Simulations in which the particle was killed at a distance of $2r_{max}$ gave results very similar to those presented in this paper. To accelerate the calculation, the step size was temporarily increased to 2 lattice units if the particle was at a distance greater than $r_{max}+10$ lattice units from the origin and was increased to 4 lattice units if the particle was at a distance of $r_{max}+20$ lattice units from the center. Similar increases to 8 lattice units at $>r_{max}+40$ and 16 lattice units at $>r_{max}+80$ were included. Similar calculations in which the step size increases were carried out at $>r_{max}+5$, $>r_{max}+10$, etc., gave very similar results to those presented in this paper indicating that these step size increases significantly reduced computer time requirements without compromising the accuracy of our results.

Fig. 2 shows a typical cluster of 11 260 particles grown on a square lattice with a sticking probability of 1.0 at nearest-neighbor sites. The random walk of the particles consists of transfers to nearest-neighbor sites as indicated in Figure 1.

Witten and Sander[4] showed that the density-density correlation function

$$C(r)=N^{-1}\sum_{r'}\rho(\vec{r}\,')\rho(\vec{r}+\vec{r}\,') \tag{1}$$

obtained in two-dimensional simulations conformed to a power-law relationship

$$C(r)\sim r^{-\alpha} \tag{2}$$

for distances r greater than a few lattice spacings but significantly less than the size of the cluster. In Eq. (1) the density $\rho(\vec{r})$ at position $\vec{r}$ is defined to be 1 for an occupied site and 0 for an unoccupied site. N is the number of particles in the cluster.

The power-law form of the density-density corre-

TABLE II. Results for diffusion-controlled cluster formation on two-dimensional square lattices with a sticking probability of 1.0 at next-nearest-neighbor sites only.

Number of particles for cluster	Radius-of-gyration exponent (β) 50%	75%	90%	95%	Density-density correlation function exponent (α)	Average coordination number
5980	0.572	0.573	0.580	0.593	0.347	2.208
4934	0.568	0.587	0.600	0.613	0.265	2.199
6973	0.598	0.582	0.574	0.579	0.272	2.219
5569	0.615	0.605	0.602	0.608	0.340	2.239
5604	0.565	0.569	0.569	0.573	0.250	2.217
Avg. 5812	0.584±0.027	0.583±0.018	0.585±0.019	0.593±0.022	0.295±0.056	2.216±0.019

lation function (Eq. 3) is consistent with a fractal[5] (Hausdorff[6]-Besicovitch) dimensionality D of $d-\alpha$ where d is the "normal" Euclidean dimensionality of the cluster. The Hausdorff dimensionality can also be obtained from the radius of gyration (R_g) which has a power-law dependence on the number of particles for sufficiently large N:

$$R_g \sim N^{\beta} . \tag{3}$$

The Hausdorff dimensionality is given by[9]

$$D_{\beta}=1/\beta . \tag{4}$$

Figure 3 shows the density-density correlation function $C(r)$ as a function of distance (r) in the form of a double-logarithmic plot.

The essentially constant slope over the range $0<\ln r<4.5$ indicates that $C(r)\sim r^{-\alpha}$ over distances from a few lattice spacings up to greater than 50 lattice spacings. The maximum radius of the cluster $r_{\max}$ is 200 lattice units. Figure 4 shows how the radius of gyration increases with increasing cluster size during the simulation of a cluster of 12 723 particles. This figure illustrates that R_g is related to N (the number of particles) according to $R_g \sim N^{\beta}$ (for large N). Table I shows the results obtained for seven clusters grown on square lattices with a sticking coefficient of 1.0 at nearest-neighbor positions. The radius-of-gyration exponents (β) shown in this table were obtained by using a "least-squares" procedure to fit the values of $\ln(N)$ and the corresponding values of $\ln(R_g)$ obtained during the addition of the last 50%, 75%, 90%, and 95% of the total particles added during cluster formation. The correlation function exponents (α) were obtained using the values of $\ln[C(r)]$ obtained from the final cluster for distances over the range $5\leq r\leq 50$ lattice units. From the correlation function exponent $\alpha=0.322\pm0.047$,[12] we obtain a corresponding Hausdorff dimensionality ($D_{\alpha}=2-\alpha$) of $D_{\alpha}=1.68\pm0.05$. Using the radius-of-gyration exponents to obtain the Hausdorff dimensionality we find $D_{\beta}=1/\beta=1.73\pm0.06$ from clusters obtained during the last 50% of cluster formation. The corresponding results for the last 75%, 90%, and 95% of particles added are 1.70 ± 0.06 (for 75%), 1.69 ± 0.05 (for 90%), and 1.69 ± 0.05 (for 95%).

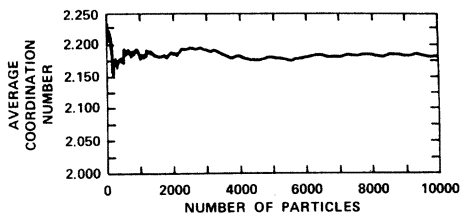

FIG. 5. Average coordination number as a function of cluster size for a two-dimensional cluster grown on a square lattice with a nearest-neighbor sticking probability of 1.0.

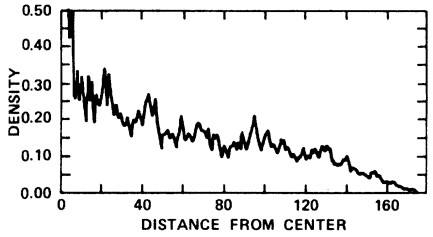

FIG. 6. Dependence of cluster density on distance from the origin for a two-dimensional cluster of 10 200 particles grown using the same conditions as earlier figures.

As the cluster grows, the average coordination number of the particles rapidly approaches an almost constant value (Fig. 5). Additional results are given in Table I. The average coordination number for large clusters is 2.191 ± 0.007.

Figure 6 shows how the cluster density decreases with increasing distance from the origin for a large cluster (10 200 particles). While there are substantial fluctuations, the overall behavior in this and other clusters is for the density to decline continuously with increasing distance from the center with no "plateau" region of constant density. This behavior is closely related to the overall decrease in density with increasing cluster size and the "fractal" characteristics of the cluster. At distances small compared to the overall size of the cluster, but large

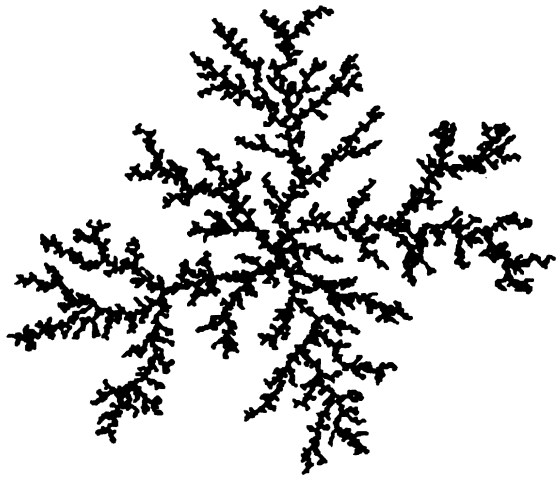

FIG. 7. Typical two-dimensional cluster of 6919 particles obtained by incorporating the "diffusing" particles into the growing cluster at next-nearest-neighbor sites only.

TABLE III. Exponents obtained from two-dimensional nonlattice simulations with a sticking probability of 1.0 at nearest-neighbor sites.

Number of particles for cluster	Radius-of-gyration exponent (β) 50%	75%	90%	95%	Density-density correlation function exponent (α)
10000	0.594	0.582	0.576	0.571	0.298
8000	0.616	0.611	0.595	0.584	0.345
8000	0.576	0.583	0.581	0.582	0.324
8000	0.563	0.568	0.570	0.569	0.312
Avg. 8500	0.587±0.032	0.586±0.025	0.581±0.015	0.577±0.011	0.320±0.028

compared to the size of a lattice site, the density should decrease with increasing distance from the center with the same power-law relationship as the density-density correlation function. While the Hausdorff dimensionality could, in principle, be obtained from the data displayed in Fig. 6 this procedure would lead to very inaccurate results.

Despite the very open nature of the cluster, few if any particles are added to the inner regions of the cluster during the later stages of growth. This is a direct consequence of the Brownian motion of the particles, i.e., almost all Brownian trajectories will intersect the outer "arms" of the growing cluster before reaching the inner regions. Consequently, growth occurs mainly in the outer regions of the cluster. This is responsible for the continuous decrease in average density as the cluster grows and leads to the fractal characteristics.

FIG. 8. Two-dimensional cluster of 10000 particles obtained on the nonlattice model for diffusion-limited cluster formation.

Figure 7 shows a typical two-dimensional cluster grown by moving the "diffusing" particle to a nearest-neighbor site during each step of the Monte Carlo calculation and incorporating the particle into the growing cluster if it reaches a *next-nearest*-neighbor site with respect to the cluster. This cluster has an even more open structure than the cluster shown in Fig. 2. However, additional growth still occurs mainly in the outer regions of the cluster, and the density-density correlation function exponent (α) and the radius-of-gyration exponent (β) have values very similar to those obtained for sticking at nearest-neighbor sites (Table II). Similar results were obtained in simulations with a sticking probability of 1.0 at both nearest-neighbor and next-nearest-neighbor sites.

Witten and Sander[4] have found that the density-density correlation function exponent (α) obtained from diffusion-limited aggregation on a two-dimensional triangular lattice ($\alpha=0.327\pm0.01$) has essentially the same value as that obtained using a square lattice (0.343 ± 0.004). To further establish the irrelevance of lattice details for the exponents α and β, nonlattice simulations of diffusion-controlled cluster formation have been carried out. In these simulations a trial in the Monte Carlo calculation consists of moving the center of a circular particle with equal probability to any point within a distance δ of its original position and testing for overlap with

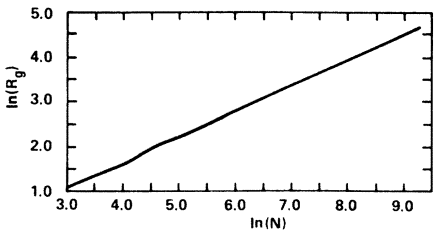

FIG. 9. Dependence of the radius of gyration (R_g) on the number of particles (N) during the growth of the clusters shown in Fig. 9.

TABLE IV. Results obtained in two-dimensional simulations with a sticking probability of 0.25 at nearest-neighbor sites.

Number of particles in cluster	Radius-of-gyration exponent (β) 50%	75%	90%	95%	Density-density correlation function exponent (x)
15907	0.593	0.586	0.576	0.566	0.293
15974	0.609	0.602	0.599	0.592	0.313
17018	0.579	0.563	0.563	0.568	0.269
15148	0.566	0.564	0.568	0.571	
14097	0.589	0.584	0.586	0.584	0.321
Avg. 15628	0.587±0.020	0.580±0.020	0.578±0.018	0.576±0.014	0.299±0.032

the growing cluster. If overlap is found, the particle is moved to the position where it first touched the cluster and is incorporated into the cluster. In our calculations the distance δ was set equal to the diameter of the circle. Smaller values of δ could have been used, but the computer time required to grow a cluster of a particular size is approximately proportional to $1/\delta^2$. Figure 8 shows a cluster of 10000 particles grown in this way with a sticking probability of 1.0. In these calculations the diffusing particle was killed and a new particle started if the particle reached a distance of 2.5 times the maximum radius from the origin. This was done to reduce computer time requirements. Nevertheless, a cluster of 10000 particles required over 20 hours of central processing unit (CPU) time to generate on a Digital Equipment Corp. VAX-11/780 computer. Values for the density-density correlation function exponent (α) and the radius-of-gyration exponent β are given in Table III, and a plot of $\ln R_g$ vs $\ln N$ where R_g is the radius of gyration and N is the number of particles is shown in Figure 9.

A comparison of Tables I—III indicates that the exponents α and β (and consequently the Hausdorff dimensionality) are independent of lattice details.

In real systems, it is possible that the diffusing particle may be repelled from the cluster at short distances or may not stick on each contact. Consequently, we have carried out simulations to explore the effects that sticking probabilities less than 1.0 have on the exponents α and β and on the morphologies of the clusters. Figure 10 shows a cluster of 9566 particles obtained in a lattice model using a sticking probability of 0.1 at next-nearest-neighbor sites only. This figure should be compared to Fig. 7 to see the effects of small sticking probabilities on cluster morphology. A small sticking probability leads to a denser cluster. Our values for the exponents α and β are shown in Table IV (sticking probability of 0.25 at nearest-neighbor sites) and Table V (sticking probability of 0.1 at next-nearest-neighbor sites). The results shown in these tables indicate that the exponents α and β are relatively insensitive to sticking coefficients over the range 0.1—1. While we had expected that α and β would be insensitive to lattice details before carrying out the simulations presented in this paper, the insensitivity to sticking probabilities was unexpected. Our results are not precise enough to determine if the sticking probability is an irrelevant parameter for

TABLE V. Results of two-dimensional simulations with a sticking probability of 0.1 at next-nearest-neighbor sites.

Number of particles in cluster	Radius-of-gyration exponent (β) 50%	75%	90%	95%	Density-density correlation function exponent (α)
9566	0.602	0.604	0.587	0.578	0.243
8745	0.599	0.578	0.572	0.572	0.271
10520	0.619	0.621	0.607	0.588	0.270
11066	0.554	0.568	0.573	0.574	0.260
10571	0.560	0.577	0.589	0.595	0.309
Avg. 10094	0.587±0.035	0.590±0.027	0.586±0.018	0.581±0.012	0.271±0.030

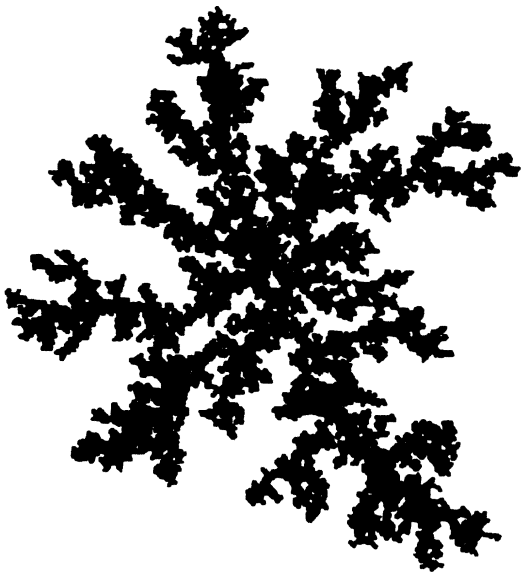

FIG. 10. Cluster of 7566 particles simulated using a lattice model with a sticking probability of 0.1 at next-nearest-neighbor positions only.

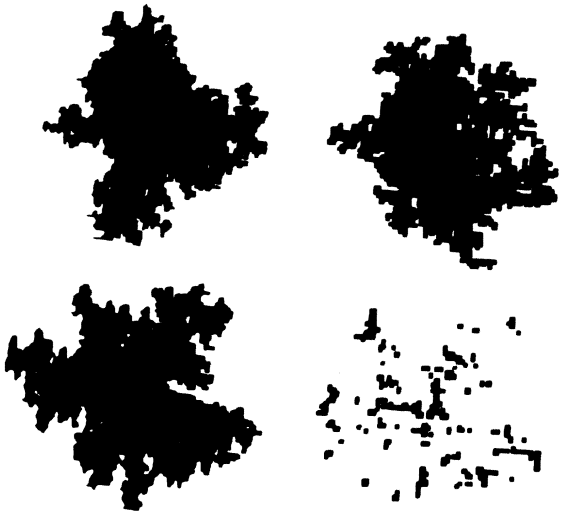

FIG. 11. Three perpendicular projections and a cross section (lower right-hand corner) for a cluster of 8257 particles grown on a simple cubic lattice.

the exponents α and β. However, the results presented in Tables I, II, IV, and V do point strongly in this direction.

THREE-DIMENSIONAL CLUSTERS

The methods used to simulate diffusion-limited cluster formation in three dimensions are analogous to those used in the two-dimensional simulations described above. As in the case of two-dimensional cluster formation, both lattice and nonlattice models have been used. In most of our three-dimensional calculations the diffusing particle was killed if it reached a distance of $2r_{\max}$ from the origin, and a new particle was started at a distance of $r_{\max}+5$ from the origin. As in our two-dimensional simulation, the step size was increased to 2 for $r > r_{\max}+10$, to 4 for $r > r_{\max}+20$, and to 8 for

TABLE VI. Experiments obtained in three-dimensional simulations of cluster growth with a sticking probability of 1.0 at nearest-neighbor sites.

Number of particles in cluster	Radius-of-gyration exponent (β) 50%	75%	90%
8257	0.420	0.416	0.409
8000	0.409	0.404	0.407
7676	0.401	0.403	0.404
6619	0.390	0.378	
7662	0.395	0.385	0.379
6608	0.421	0.408	0.394
10000	0.415	0.415	0.406
7805	0.382	0.377	0.382
7870	0.411	0.404	0.403
6896	0.381	0.390	0.393
8787	0.373	0.380	0.394
9219	0.393	0.388	0.389
9236	0.398	0.396	0.397
7235	0.429	0.429	0.424
6518	0.416	0.430	0.444
7917	0.404	0.397	0.397
Avg. 7899	0.402±0.009	0.400±0.009	0.401±0.009

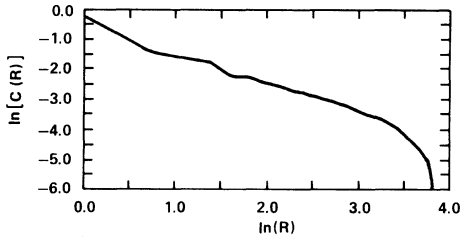

FIG. 12. Density-density correlation function $[C(r)]$ for a three-dimensional cluster of 7762 particles grown under the conditions used to obtain Fig. 11.

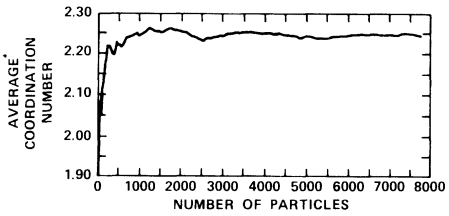

FIG. 14. Dependence of average coordination number on cluster size during the formation of a cluster of 7870 particles.

$r > r_{max} + 40$, where r is the distance of the diffusing particle from the origin.

Figure 11 shows a typical cluster of 8257 particles grown on a simple cubic lattice with a sticking probability of 1.0 at nearest-neighbor positions. The three-dimensional clusters grown under diffusion-limited conditions have a low average density which decreases with increasing cluster size. As in the case of the two-dimensional clusters, growth occurs mainly at the outer regions of the clusters despite their very open structure.

The density-density correlation function $C(r)$ for a cluster of 7762 particles is shown in Figure 12. It is not possible to simulate three-dimensional clusters (and clusters of higher dimensionality) which are large enough to obtain a linear region in plots of $\ln[C(r)]$ vs $\ln(r)$ over a range of distances which are both larger than a few lattice spacings and significantly smaller than the overall dimensions of the cluster. Attempts to fit portions of $\ln C(r)$ vs $\ln(r)$ plots (such as Fig. 12) by a straight line give results which are clearly dependent on the size of the clusters even for clusters of 10000 particles, i.e., the apparent value of the density-density correlation function exponent (α) decreases with increasing cluster size. Fortunately, the values of the radius-of-gyration exponents (β) do not seem to be nearly as sensitive to finite-size effects, and we have relied on the dependence of the radius of gyration (R_g) on cluster size (N) to obtain the Hausdorff dimensionality via the radius-of-gyration exponent (β). Figure 13 shows how the radius of gyration increases with increasing cluster size during the formation of a cluster of 4883 particles. After the first few hundred particles have been added, we find that $R_g \sim N^{\beta}$ ($\beta \approx 0.4$). The results obtained from 12 clusters containing from 6608 to 10000 particles are summarized in Table VI. The results shown in Table VI indicate that $R_g \sim N^{\beta}$ with β approximately equal to 0.4. The corresponding Hausdorff dimensionality is approximately 2.5. As the cluster size increases, the average coordination number of the particles in the cluster rapidly approaches an essentially constant value (Fig. 14). From nine clusters (average 7900 particles per cluster), we find that the average coordination number is 2.251 ± 0.006.

One quantity which can often be measured in real clusters is the area of a projection of the cluster on a plane. Figure 15 shows how the projected areas depend on cluster size during the growth of a cluster of 7870 particles. From Fig. 15 it can be seen that the projected areas depend on cluster size according to the power-law relationship $P \sim N^{\gamma}$ in the limit of large N. From seven clusters (average 7600 particles per cluster), we find that $\gamma = 0.870 \pm 0.017$ using the last 50% of the clusters formed. Using the last 75%, 90%, and 95% of clusters formed during the simulations, we find $\gamma = 0.864 \pm 0.010$, 0.861 ± 0.004,

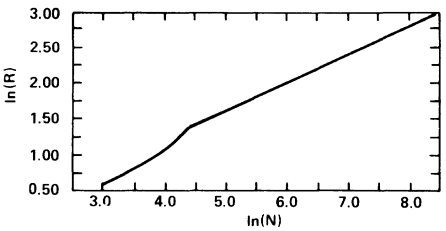

FIG. 13. Dependence of radius of gyration (R_g) on cluster size (N) during the formation of a cluster of 4883 particles on a simple cubic lattice with a sticking probability of 1.0 at nearest-neighbor sites.

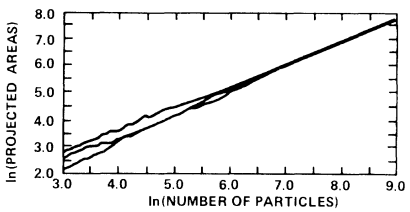

FIG. 15. Dependence of projected areas on cluster size for a cluster of 7870 particles. Areas are the projections on three mutually perpendicular planes calculated during the growth of the cluster.

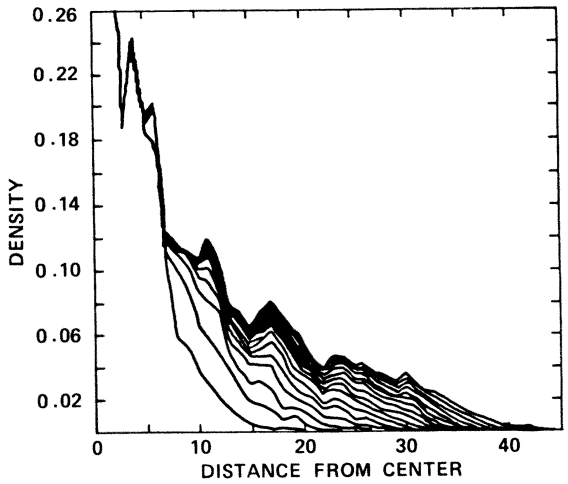

FIG. 16. Density profiles during the growth of a three-dimensional cluster. Density profiles are shown at stages where the cluster has grown to a size of 500,1000,...,8000 particles.

and 0.861 ± 0.008, respectively. The uncertainty estimates[12] are only slightly reduced if the three projected areas are averaged for each cluster.

Figure 16 shows the density profile at several stages during the growth of a three-dimensional cluster. As in the case of two-dimensional clusters grown under diffusion-limited conditions, the cluster density decreases monotonically with increasing distance from the origin (if fluctuations are ignored). This figure also illustrates that particles are not added to the central portions of the cluster during the later stages of growth. In Fig. 17 the number of particles at a distance of $r \pm 0.5$ (lattice units) are shown as a function of r during the growth of a three-dimensional cluster.

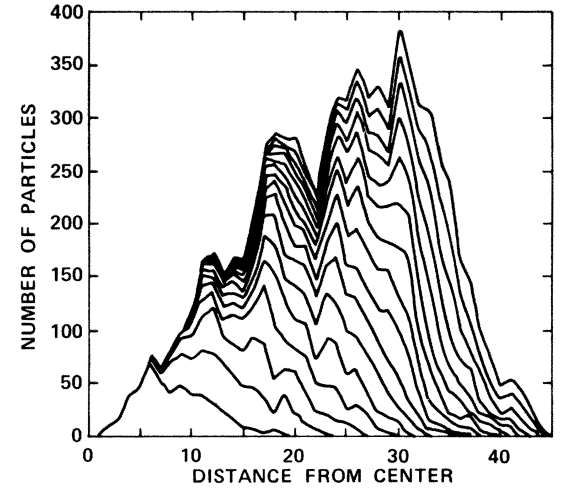

FIG. 17. Number of particles in a spherical shell between $r-0.5$ and $r+0.5$ during the growth of a cluster in three-dimensional space. Cluster sizes used in this figure are 500,1000,...,8000 particles.

TABLE VII. Results of three-dimensional simulations of clusters grown on a simple cubic lattice with a sticking coefficient of 0.25.

Number of particles in cluster	Radius-of-gyration exponent (β) 50%	75%	90%
10000	0.379	0.379	0.381
9320	0.417	0.412	0.407
15000	0.408	0.402	0.394
15000	0.392	0.382	0.384
12179	0.430	0.421	0.403
Avg. 12300	0.405±0.025	0.401±0.019	0.394±0.014

Simulations have been carried out to investigate the effects of sticking probabilities less than 1.0 on the radius-of-gyration exponent (β). Our results are shown in Table VII for a sticking probability of 0.25. A comparison of Tables VI and VII indicates that sticking coefficients of 1.0 and 0.25 give essentially the same values for the radius-of-gyration exponent (β). Consequently, we may conclude that the Hausdorff dimensionality for diffusion-controlled clusters grown in three-dimensional space is insensitive to the sticking probability. However, reducing the sticking probability from 1.0 to 0.25 does change the projected area exponent γ. For the five clusters shown in Table VII we find $\gamma = 0.831 \pm 0.018$, 0.829 ± 0.016, 0.830 ± 0.014, and 0.830 ± 0.014 from analysis of the last 50%, 75%, 90%, and 95% of the clusters formed during the simulations, respectively. The average coordination

TABLE VIII. Radius-of-gyration exponents obtained in nonlattice simulations of diffusion-limited cluster formation in three-dimensional space.

Number of particles	Radius-of-gyration exponent (β) 50%	75%	90%
2500	0.375	0.394	0.408
8000	0.418	0.412	0.406
2500	0.436	0.424	0.420
5000	0.390	0.402	0.398
10000	0.382	0.384	0.388
8000	0.392	0.394	0.402
10000	0.389	0.390	0.393
Avg. 6571	0.397±0.020	0.400±0.013	0.402±0.010

TABLE IX. Radius-of-gyration exponents obtained in four-dimensional simulations of diffusion-controlled cluster formation on a simple hypercubic lattice. The nearest-neighbor sticking coefficient is 1.0.

Number of particles	Radius-of-gyration exponent (β) 50%	75%	90%
2209	0.303	0.297	
1841	0.288	0.293	
682	0.274	0.279	
1021	0.325	0.286	
1617	0.289	0.289	
1717	0.303	0.331	
901	0.287	0.306	
1256	0.296	0.289	
1717	0.334	0.339	
1303	0.281	0.309	
2616	0.323	0.324	0.324
1857	0.286	0.282	0.279
1534	0.324	0.330	0.315
1589	0.299	0.307	0.311
2500	0.304	0.301	0.310
5000	0.304	0.310	0.303
5000	0.283	0.288	0.297
5000	0.280	0.279	0.283
5000	0.304	0.301	0.308
Avg. 2335	0.299±0.009	0.302±0.009	0.303±0.011

TABLE X. Radius-of-gyration exponent obtained from simulation of diffusion-controlled cluster formation using a five-dimensional hypercubic lattice and a nearest-neighbor sticking coefficient of 1.0.

Number of particles	Radius-of-gyration exponent (β) 50%	75%
2000	0.240	0.228
1000	0.238	0.262
2500	0.231	0.232
1460	0.251	0.246
2500	0.225	0.226
2500	0.228	0.233
2500	0.253	0.248
4000[a]	0.233	0.246
5000[a]	0.240	0.254
4000[a]	0.246	0.231
5000[a]	0.242	0.240
2500[a]	0.224	0.213
Avg. 2914	0.238±0.006	0.238±0.009

[a]"Kill radius" equals $1.5r_{max}$; "doubling radii" equals $r_{max}+5$, $r_{max}+10$, and $r_{max}+20$.

number is, of course, sensitive to the sticking probability (S). For $S=0.25$, the value of 2.514±0.018 is obtained.

Since three-dimensional clusters will be opaque in the limit of large N ($d-D<1$) the exponents β and γ should be related by $\gamma=2\beta$. Consequently, the projected area exponents γ provide another estimate of the Hausdorff dimensionality of the cluster. For three-dimensional clusters grown with a sticking probability of 1.0 our value for γ (~ 0.865) implies a Hausdorff dimensionality of ~ 2.31. Similarly, the value of the projected area exponent obtained from clusters grown with a sticking probability of 0.25($\gamma \sim 0.83$) can be used to estimate a Hausdorff dimensionality of ~ 2.41. These results are about 8% and 4% smaller than the results obtained from the radius-of-gyration exponent (β) for $S=1.0$ and 0.25, respectively. The difference between these estimates is attributed to finite-size effects. Since even clusters of 10000 particles are not large enough to be fully opaque, the projected area exponent will be larger than its $N \to \infty$ limiting value. Consequently, the apparent Hausdorff dimensionality should increase with increasing N. While this would bring the values for D obtained from the exponents β and γ into closer agreement, the possibility that γ may not have reached its limiting value at $N=10000$ may also be proposed for the radius-of-gyration exponent β. It should also be noted, however, that the differences between the values obtained for the Hausdorff dimensionality from the radius-of-gyration and projected area exponents are not very much larger than their statistical uncertainties.

To help establish the anticipated independence of the radius-of-gyration exponent (β) on lattice details, a nonlattice model which simulates the diffusion of spherical particles has been developed. For the simulation of the larger clusters obtained using this method (8000 or 10000 particles), the maximum step size is doubled to 2 particle radii at $r > r_{max}+7$ and doubled again at $r > r_{max}+15$ and

TABLE XI. Radius-of-gyration exponents (β) obtained from simulations of diffusion-limited cluster formation using a six-dimensional hypercubic lattice.

Number of particles	Radius-of-gyration exponent (β) 50%	75%
2000	0.241	0.239
2000	0.207	0.202
5000	0.183	0.182
8000	0.193	0.193
10000	0.193	0.186

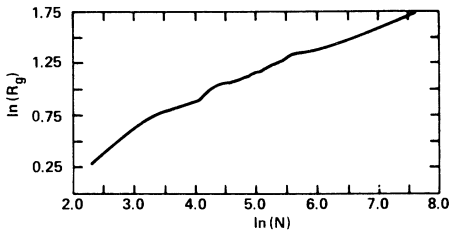

FIG. 18. Dependence of $\ln(R_g)$ on $\ln(N)$ during the formation of a cluster of 2000 particles in a five-dimensional hypercubic lattice.

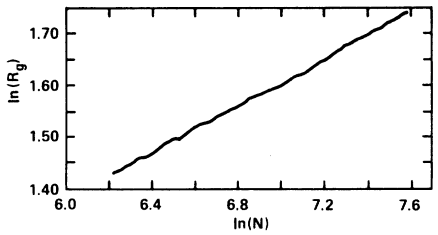

FIG. 19. This figure shows an expansion of that portion of Fig. 18 which is used to obtain the radius-of-gyration exponent (β).

at $r > r_{max} + 30$. The results obtained in these simulations are given in Table VIII. The sticking probability in these simulations is 1.0. A comparison of Tables VI and VIII indicates that the radius-of-gyration exponent is not sensitive to lattice details in three-dimensional simulations.

FOUR-DIMENSIONAL CLUSTERS

Diffusion-controlled cluster formation in four-dimensional space was simulated using a lattice model very similar to those described above. In these simulations the particle was started at a random point on a hyperspherical surface of radius $r_{max}+4$ lattice units and killed at a distance greater than $2r_{max}$ units (except in the very early stages of the simulation where the particle was killed if it reached a position more than 12 lattice units from the origin). As in calculations in spaces of lower dimensionality, the step size was temporarily doubled at positions greater than $r_{max}+10$ from the origin and doubled again if $r > r_{max}+20$, etc. Fifteen clusters with an average of 1600 particles per cluster were simulated in this way (Table IX) leading to the result $\beta = 0.304 \pm 0.011$ ($D_\beta = 3.29 \pm 0.12$) using the last 50% of the clusters formed in each simulation.

Somewhat larger clusters could be grown by storing only the coordinates of occupied lattice sites in the computer. Four clusters with 5000 particles each were generated in this way. For these four clusters we find $\beta = 0.293 \pm 0.021$ from the last 50% of the clusters formed in the simulations. Similarly, $\beta(75\%) = 0.295 \pm 0.022$ and $\beta(90\%) = 0.298 \pm 0.017$.

SIMULATION OF DIFFUSION-CONTROLLED CLUSTER FORMATION ON A FIVE-DIMENSIONAL HYPERCUBIC LATTICE

Cluster formation was simulated in five-dimensional space using the same method which was used to simulate the larger clusters on a four-dimensional lattice (see above). Particles were started at a distance $r_{max}+3$ from the origin and killed if

TABLE XII. Hausdorff dimensionality (D) of clusters grown under diffusion-controlled conditions. $2d$ through $6d$ stand for two- through six-dimensional, respectively; NN, nearest neighbor; NNN, next nearest neighbor; NL, nonlattice; $\frac{5}{6} = 0.8333$.

Model	D (50%)	D (75%)	D/d (50%)	D/d (75%)
$2d$, S(NN)=1.0	1.73±0.06	1.70±0.06	0.87±0.03	0.85±0.03
$2d$, S(NNN)=1.0	1.71±0.08	1.72±0.05	0.86±0.04	0.86±0.03
$2d$, S(NL)=1.0	1.70±0.09	1.71±0.07	0.86±0.05	0.86±0.03
$2d$, S(NN)=0.25	1.70±0.06	1.72±0.06	0.85±0.03	0.86±0.03
$2d$, S(NNN)=0.1	1.70±0.10	1.69±0.08	0.85±0.05	0.85±0.04
$3d$, S(NN)=1.0	2.51±0.06	2.53±0.06	0.84±0.02	0.84±0.02
$3d$, S(NN)=0.25	2.47±0.15	2.49±0.12	0.82±0.05	0.83±0.04
$3d$, S(NL)=1.0	2.52±0.13	2.50±0.08	0.84±0.04	0.83±0.03
$4d$, S(NN)=1.0	3.34±0.10	3.31±0.10	0.84±0.03	0.83±0.03
$5d$, S(NN)=1.0	4.20±0.11	4.20±0.16	0.84±0.02	0.84±0.03
$6d$, S(NN)=1.0	~5.3	~5.35	~0.88	~0.89

they reached a position greater than $2r_{max}$ from the origin. In this way seven clusters with an average of 2066 particles per cluster were grown. From these seven clusters, the results $\beta(50\%)=0.238\pm0.010$ were obtained using the last 50% of clusters formed. Similarly, we found that $\beta(75\%)=0.239\pm0.012$ from the last 75%. Since the formation of a cluster of 2500 particles took more than ten hours of CPU time, the distance at which particles were killed was reduced to $1.5r_{max}$, and the step size was temporarily doubled at $r>r_{max}+5$ and at $r>r_{max}+10$ and $r>r_{max}+20$ to simulate larger clusters (Table X). Apart from the desire to grow larger clusters on a five-dimensional lattice, these calculations were also motivated by the need to demonstrate that a "kill radius" of $1.5r_{max}$ and doubling radii of $r_{max}+5$, $r_{max}+10$, and $r_{max}+20$ would give accurate results in our six-dimensional simulations. In six-dimensional simulations the errors caused by these approximations, used to reduce computer time, should be significantly smaller than they are in five dimensions.

Figure 18 shows how the radius of gyration increases with increasing cluster size during the formation of a five-dimensional cluster of 2000 particles. It should be noted that we are interested mainly in the dependence of the radius of gyration on cluster size in the limit of large cluster sizes. Figure 19 shows a plot of $\ln(R_g)$ vs $\ln(N)$ during the addition of the last 1500 particles. It is this portion of the curve shown in Fig. 18 which is used to obtain β.

SIX-DIMENSIONAL CLUSTERS

The parameters used to simulate diffusion-controlled cluster formation on a six-dimensional hypercubic lattice are discussed in the previous section. The results of these calculations are shown in Table XI. Unfortunately, we were not able to grow a sufficiently large number of large clusters to obtain a reliable result for the Hausdorff dimensionality (D). However, our results do indicate that $D<d$.

DISCUSSION

One of the most important results of these simulations is the relationship between the Hausdorff dimensionality (D) and the Euclidean dimensionality (d) shown in Table XII. In all cases ($d=2$–6) our results are consistent with the relationship $D\approx 5d/6$. In the absence of theoretical understanding of the Hausdorff dimensionality of clusters obtained by diffusion-controlled growth there is no reason to expect that D and d will be related by a simple constant such as $\frac{5}{6}$. The results presented in this paper are numerical estimates of the Hausdorff dimensionality which become increasingly more unreliable as the dimensionality increases (despite the small statistical uncertainties). We know that the relationship $D\approx 5d/6$ is not correct for $d=1$ ($D=d=1$). Similarly, for $d>12$, $D\approx 5d/6$ implies that $d-D>2$. Since a random walk has a Hausdorff dimensionality of 2 the cluster would become transparent to a random walk if $d-D>2$. This would allow particles to enter into the central regions of the cluster thus increasing the Hausdorff dimensionality of the cluster until $d-D\leq 2$. The relationship $D\approx 5d/6$ is simply a convenient way of summarizing our results.

Since relationships of the type $R_g\sim N^{\beta}$ are expected to be valid only in the limit $N\rightarrow\infty$, we have generated the largest clusters which were practical in our VAX-11/780 computer. Results obtained for clusters of various sizes (or at various stages during the formation of a large cluster) indicate that the values we have obtained for the radius-of-gyration exponents are close to their limiting values. However, it is possible that similar simulations which generated *much* larger clusters would lead to different results. Unfortunately, it is unlikely that such simulations will be possible in the near future. The 4–8% difference between the values for the Hausdorff dimensionality obtained from the radius-of-gyration exponent (β) and the projected area exponent (γ) for large clusters grown on a three-dimensional lattice indicates that the $N\rightarrow\infty$ limit may not have been reached in these simulations. While we have reasons for believing that it is the projected area exponent (γ) which is still changing with increasing N the possibility the radius-of-gyration exponent β will also change as $N\rightarrow\infty$ must also be recognized. The average density in the outer regions of the cluster falls more rapidly with increasing distance from the center than in the inner regions where the power law $\rho(r)\sim r^{D-d}$ is obeyed. At higher dimensionalities this outer region becomes a larger and larger fraction of the total cluster (for a fixed number of particles). Consequently, finite-size effects may become more important for clusters grown in higher-dimensional lattices. Despite these uncertainties we have included our results for clusters grown in four, five, and six dimensions in this paper since our results for $d=4$–6 are the only ones available at this time. The major objective of this paper is to present results for simulations of diffusion-controlled cluster formation in two- and three-dimensional space for which these uncertainties are relatively small.

In spite of the large cluster sizes used in this work, the variability in the results obtained from calculation to calculation was surprisingly large.

This may be related to the fact that the calculations described here can be regarded as a simulation of the dendritic growth instability in the limit where fluctuations are dominant.[4,13] Regions of the cluster near the perimeter "shield" the inner portions of the cluster and grow preferentially. Fluctuations in the cluster perimeter are enhanced by the diffusion-controlled growth mechanism and tend to be amplified. For this reason, the shape of the cluster at late stages is strongly dependent on the shape at much earlier stages. This is illustrated in Fig. 2, which shows a typical cluster formed by diffusion-controlled aggregation.

[1]S. K. Friedlander, *Smoke, Dust and Haze Fundamentals of Aerosol Behavior* (Wiley, New York, 1977).

[2]M. J. Vold, J. Colloid Sci. 18, 684 (1963).

[3]H. P. Hutchison and D. M. Sutherland, Nature 206, 1036 (1965); D. N. Sutherland, *ibid.* 226, 1241 (1970); D. N. Sutherland, J. Colloid Interface Sci. 22, 300 (1966); 25, 373 (1967); D. N. Sutherland and I. Goodarz-Nia, Chem. Eng. Sci. 26, 2071 (1971).

[4]T. A. Witten and L. M. Sander, Phys. Rev. Lett. 47, 1400 (1981).

[5]B. B. Mandelbrot, *Fractals, Form, Chance and Dimension* (Freeman, San Francisco, 1977).

[6]F. Hausdorff, Math. Ann. 79, 157 (1919).

[7]P. Meakin, Phys. Rev. A 27, 604 (1983).

[8]D. S. McKenzie, Phys. Rep. C 27, 35 (1976); P. J. Flory, *Principles of Polymer Chemistry* (Cornell University Press, Ithaca, N.Y., 1953); P. G. de Gennes, *Scaling Concepts in Polymer Physics* (Cornell University Press, Ithaca, N.Y., 1979).

[9]H. E. Stanley, J. Phys. A 10, L211 (1977).

[10]S. Kirkpatrick, Rev. Mod. Phys. 45, 574 (1973); H. Peters, D. Stauffer, H. P. Hölters, and K. Loewich, Z. Phys. B 34, 399 (1979); P. L. Leath, Phys. Rev. B 14, 5046 (1976); D. Stauffer, Phys. Rev. Lett. 41, 1333 (1978); D. Stauffer, Phys. Rep. 54, 3 (1979); J. W. Essam, Rep. Prog. Phys. 43, 833 (1980); C. Domb, T. Schneider, and E. Stoll, J. Phys. A 8, L90-4 (1975).

[11]H. E. Stanley, *Introduction to Phase Transitions and Critical Phenomena* (Oxford University Press, New York, 1971).

[12]The error ranges given in this paper are 95% confidence limits. Systematic errors arising from finite-size effects, nonrandom distribution of pseudorandom numbers, etc., are not included.

[13]J. S. Langer and H. Müller-Krumbhaar, Acta Metal. 26, 1681 (1978); 26, 1689 (1978); 26, 1697 (1978); H. Müller-Krumbhaar and J. S. Langer, Acta Metal. 29, 145 (1981); J. S. Langer, *Nonlinear Phenomena at Phase Transitions and Instabilities,* NATO Advanced Study Institute, Geilo, Norway, 1981 (Plenum, New York, 1982); J. S. Langer, Rev. Mod. Phys. 52, 1 (1980).